Mitochondrial Genomics and Proteomics of *Yarrowia lipolytica*

Stefan Kerscher and Ulrich Brandt

Abstract In recent years, we have developed the obligate aerobic yeast *Y. lipolytica* as a model system to analyse respiratory chain complex I (proton pumping NADH:ubiquinone oxidoreductase). Our studies were aimed at exploring structural and functional constraints for the reaction mechanism at the catalytic core of this giant enzyme, defined as the site where ubiquinone reduction couples to proton translocation. Extensive genomic and proteomic analyses of *Y. lipolytica* mitochondria resulted in the discovery of 41 different complex I subunits, encoded both by the mitochondrial and the nuclear genome. Most of the subunits of complex V (ATP synthase) and a protein specifically involved in complex I iron–sulfur cluster assembly were also described. Novel gel-electrophoretic separation techniques and analytical methods, especially laser-induced liquid bead ion desorption (LILBID) mass spectrometry, developed for these purposes, have great potential as useful tools for obtaining molecular fingerprints of large protein assemblies.

S. Kerscher
Center for Membrane Proteomics, Cluster of Excellence Frankfurt "Macromolecular Complexes", Molekulare Bioenergetik, Fachbereich Medizin, Goethe-Universität, 60590 Frankfurt am Main, Germany

U. Brandt (✉)
ZBC, Cluster of Excellence Frankfurt "Macromolecular Complexes", Molekulare Bioenergetik, Fachbereich Medizin, Goethe-Universität, Frankfurt am Main, Germany

Present address: Nijmegen Centre for Mitochondrial Disorders (NCMD), Radboud University Medical Centre Geert Groteplein-Zuid 10, 6525 GA Nijmegen, The Netherlands
e-mail: u.brandt@cukz.umcn.nl

G. Barth (ed.), *Yarrowia lipolytica*, Microbiology Monographs 24,
DOI 10.1007/978-3-642-38320-5_2, © Springer-Verlag Berlin Heidelberg 2013

Contents

1 Introduction

In recent years, the obligate aerobic yeast *Yarrowia lipolytica* has been firmly established as a powerful yeast genetic model system for the analysis of respiratory chain complex I. Due to the intricate composition of this multi-subunit enzyme, this work was accompanied by large-scale genomic and proteomic analyses of *Y. lipolytica* mitochondria. In this chapter, we are going to review these efforts, with a special emphasis on novel analytical methods that were developed in the course of these studies.

Many questions on complex I remain unanswered. Only recently the complex was studied by X-ray crystallography (Hunte et al. 2010; Efremov et al. 2010; Baradaran et al. 2013), and the reaction mechanism is far from being understood. This lack of information is untenable in view of the vital position of complex I in human metabolism, as illustrated by the fact that inherited and acquired complex I defects cause severe, progressive and often fatal disorders, with Leigh syndrome as the most typical clinical manifestation (see below).

While *Saccharomyces cerevisiae* has proven an excellent model system for the genetic analysis of numerous topics in cell biology, the enzymatic machinery of this species, as a consequence of its adaptation to the fermentative lifestyle (Lagunas 1986), displays several peculiar features, including the lack of respiratory chain complex I. The resulting inapplicability of the *S. cerevisiae* model system certainly is among the reasons why the analysis of complex I is still lagging behind the work on other complexes of the respiratory chain.

We therefore set out to establish a yeast model system for the analysis of complex I. The obligate aerobic yeast *Y. lipolytica* was chosen since its genetics are quite well advanced (Barth and Gaillardin 1996), as it combines heterothallism and two stable mating types with the availability of replicative and integrative plasmids and several easily scorable metabolic and resistance markers. The genomic sequence of *Y. lipolytica* has been analysed by the Genolevures consortium (Dujon et al. 2004).

The most widely accepted reference system for eukaryotic complex I, studied extensively on the proteomic level, is complex I from bovine heart. Evolutionary

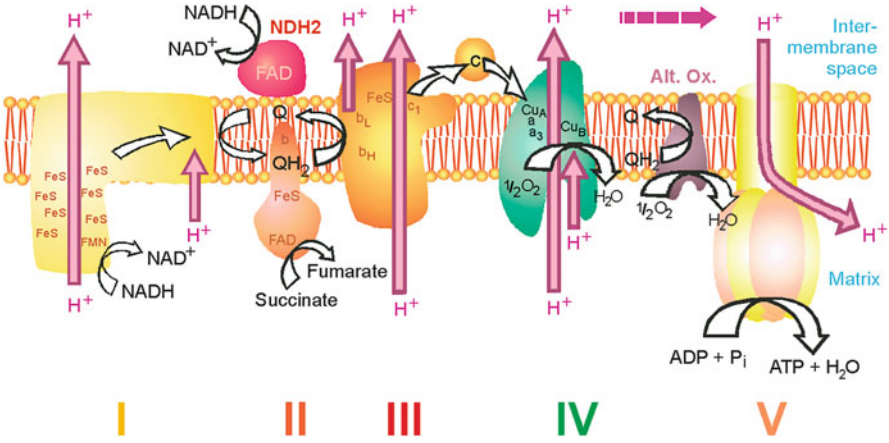

Fig. 1 Respiratory chain of *Y. lipolytica*. Schematic representation of the respiratory chain of *Y. lipolytica*. Substrate flow is indicated by *white* and proton pumping by *pink arrows*. I, II, III, IV, V, respiratory chain complexes I–V; a, a_3, heme *a* and a_3; Alt. Ox., alternative oxidase; b, heme *b*; b_L, b_H, low and high potential heme *b*; c, c_1, heme *c* and c_1; Cu_A, Cu_B, copper centre A and B; FeS, iron–sulfur cluster; Q, ubiquinone; QH_2, reduced ubiquinone; NDH2, alternative NADH dehydrogenase

conserved subunits of *Y. lipolytica* complex I were thus named after their bovine heart homologues. In addition, a few yeast-/fungus-specific subunits were found.

2 The Mitochondrial Respiratory Chain of *Y. lipolytica*

The respiratory chain of *Y. lipolytica* mitochondria does possess not only complex I but also all other respiratory chain complexes found in mammals including humans (Fig. 1), namely, complex II (succinate:ubiquinone oxidoreductase), complex III (ubiquinol:cytochrome *c* oxidoreductase), complex IV (cytochrome *c* oxidase) and complex V (ATP synthase). The ubiquinone species employed by *Y. lipolytica*, termed Q_9, has a nine-unit isoprenoid side chain (Kurtzman 1994). This is closer to $Q_{9–11}$ found in mammals than to Q_6 found in *S. cerevisiae*. Also, the phospholipid composition of mitochondrial membrane fractions (Arthur and Watson 1976) was found to be similar to that of mammalian mitochondria.

As in human mitochondria, complexes I, III and IV, by pumping protons into the intermembrane space, build up a transmembrane proton gradient which is then used to drive ATP synthesis by complex V. Besides these complexes, the respiratory chain of *Y. lipolytica* mitochondria also comprises so-called alternative enzymes, as typically found in plants and fungi. Alternative NADH dehydrogenase (NDH2) carries out the same redox reaction as complex I (Kerscher 2000; Melo et al. 2004), while alternative terminal oxidase (AOX) bypasses complexes III and IV (Joseph-Horne et al. 2001). Both enzymes consist of a single subunit only and do not pump protons. NDH2 contains a non-covalently bound FAD molecule as sole redox

prosthetic group. Alternative NADH dehydrogenases have been found in archae- and eubacteria, in protists, plants and fungi. As these enzymes can reside on either the inner or the outer face of the mitochondrial inner membrane, eukaryotic alternative NADH dehydrogenases can be classified as internal or external. For example, *S. cerevisiae* mitochondria possess two external and one internal alternative enzyme (Marres et al. 1991; Luttik et al. 1998). Only the internal form of NDH2 confers resistance to complex I inhibitors like DQA and rotenone (Kerscher et al. 2001b).

AOX which occurs in plants and fungi contains a di-iron active centre and confers resistance to inhibitors of complexes III and IV. AOX activity is detectable in *Y. lipolytica* cells growing in the presence of antimycin A or cyanide. In *Y. lipolytica* cultures growing in the absence of such poisons, AOX is expressed in stationary phase cells but in an inactive form that only becomes activated in conditions that elevate cellular AMP levels (Medentsev and Akimenko 1999).

Studying the properties of the alternative NADH dehydrogenase of *Y. lipolytica* proved to be of vital importance for establishing this yeast as a model system for complex I research (Kerscher et al. 1999). When we first tried to sporulate diploid strains heterozygous for a deletion allele for one of the seven nuclear encoded central subunits of complex I, no viable haploid strains carrying the deletion allele could be identified among the progeny. We concluded that, in contrast to other fungi like *Neurospora crassa* and *Aspergillus spec*. where complex I null mutants had been generated before, complex I function was essential for survival of standard laboratory strains of *Y. lipolytica*. At that time, it appeared that genetic analysis of complex I using *Y. lipolytica* was impossible.

However, a useful hint to a solution for this problem was found when the alternative NADH dehydrogenase activity of *Y. lipolytica* was analysed in more detail. A comparison of intact and permeabilised *Y. lipolytica* mitochondria clearly demonstrated that alternative NADH dehydrogenase activity in this yeast was exclusively due to an external enzyme. Following deletion of the NDH2 gene, alternative NADH dehydrogenase activity was completely abolished (Kerscher et al. 1999).

Next, we created a gene fusion in which a truncated NDH2 open reading frame was fused to the sequence encoding the mitochondrial targeting sequence of the 75-kDa subunit of *Y. lipolytica* complex I. The construct was randomly integrated into the *Y. lipolytica* genome, and transgenic colonies could be isolated by virtue of their ability to grow in the presence of the complex I inhibitor DQA. Thus, the internal version of *Y. lipolytica* NDH2, termed NDH2i, was able to substitute for the NADH dehydrogenase function of complex I (Kerscher et al. 2001b). Its presence permitted the deletion of nuclear genes for essential subunits of complex I, which could then be complemented with plasmid-borne site-directed mutant copies of the respective genes.

It should be noted that a further alternative NADH dehydrogenase gene (YALI0E05599g) was detected in *Y. lipolytica* during the course of the genome project. Its functional significance remains unclear since a catalytic activity corresponding to the enzyme encoded by this gene has not been reported yet.

Table 1 Assignment of EPR signals to the iron–sulfur clusters of complex I

		EPR signal assignment	
Cluster type	Subunit name (*Bos taurus*)	Traditional	Revised
Fe_2S_2	24 kDa	N1a	N1a
Fe_4S_4	51 kDa	N3	N3
Fe_2S_2	75 kDa	N1b	N1b
Fe_4S_4	75 kDa	N4	N5
Fe_4S_4	75 kDa	N5	Not detectable
Fe_4S_4	TYKY	N6a	N4
Fe_4S_4	TYKY	N6b	Not detectable
Fe_4S_4	PSST	N2	N2

Adapted from Yakovlev et al. (2007) and Roessler et al. (2010)

3 Characteristic Features of Complex I

Among the reasons why mitochondria as endosymbionts are of prime value for their hosts, their superior capability of ATP production by utilisation of oxygen holds one of the top ranks. Complex I (NADH:ubiquinone oxidoreductase) in mammals makes a major contribution (up to 40 %, depending on metabolic conditions) to the proton gradient across the inner mitochondrial membrane and hence to oxidative phosphorylation (Brandt 2006). The transfer of two electrons from NADH to ubiquinone is coupled to the translocation of four protons (Galkin et al. 2001, 2006). Complex I is a huge multiprotein assembly, composed of 45 subunits in mammals (Carroll et al. 2006) and around 40 subunits in fungi (Morgner et al. 2008), with a total molecular mass in the range of one million Dalton. The enzyme is L shaped with two arms of similar length and girth, oriented perpendicular to each other, a hydrophobic arm imbedded in the respiratory membrane and a hydrophilic peripheral arm protruding into the mitochondrial matrix (Radermacher et al. 2006). The peripheral arm carries all redox prosthetic groups, namely, one FMN and eight iron–sulfur clusters, two of which are of the binuclear and six of the tetranuclear type (Table 1; Sazanov and Hinchliffe 2006); the membrane arm harbours the proton pump.

Many bacteria, including *Escherichia coli*, possess a "minimal form" of complex I that is composed of 14 subunits only, with a total molecular mass of about 550 kDa (Friedrich 1998; Yano and Yagi 1999). Seven subunits each make up the peripheral and the membrane arm, respectively. All of them have homologues in eukaryotic complex I, termed "central subunits," since obviously they are sufficient to carry out the bioenergetic function of complex I. In mammals and fungi, the seven central subunits of the peripheral arm are nuclear coded, while the seven central subunits of the membrane arm are mitochondrially coded (Table 2). The function of the "accessory subunits" of eukaryotic complex I, all of which are nuclear coded, is largely unknown (see below).

While the subunit composition of bacterial complex I is much simpler and its molecular mass is markedly lower than that of the eukaryotic enzymes, using the

Table 2 Subunits of *Y. lipolytica* mitochondrial complex I

Subunit					M_r[c]		Prosth. groups		LILBID	
No	Gene	Protein	TMDs[a]	N-terminal sequence[b]	Precursor	Mature	Type	M_r	m/z	Remarks
Central nuclear coded										
1	NUAM	75-kDa	0/0	AEIELT[f]	78,997.2	75,198.7	$Fe_{10}S_{10}$	879.2	75.2	
2	NUBM	51-kDa	0/0	ATTQDA[f]	53,755.6	51,660.0	Fe_4S_4	351.7	51.7	R1
							FMN	456.4		
3	NUCM	49-kDa	0/0	ATTALP[f]	52,430.0	49,945.0	–	–	49.9	R3
4	NUGM[d]	30-kDa	0/0	QAAPSS[f]	33,594.9	30,476.2	–	–	30.5	
5	NUHM	24-kDa	0/0	IVSVHR[g]	27,216.4	24,068.6	Fe_2S_2	175.8	24.3	
6	NUIM	TYKY	1/0	APATDS[g]	25,651.3	22,321.3	Fe_8S_8	703.4	22.3	
7	NUKM	PSST	0/0	SAPAGT[f]	23,430.2	20,425.6	Fe_4S_4	351.7	20.2	R2,3
Sum						274,095.4		2,918.2		
Central mitochondrially coded										
8	NU1M	ND1	10/10			38,347.7			38.3	
9	NU2M	ND2	14/13			53,331.9			53.2	
10	NU3M	ND3	3/3			14,470.5			14.5	
11	NU4M	ND4	13/12			54,481.2			54.4	
12	NU5M	ND5	18/16			73,705.4			73.5	
13	NU6M	ND6	5/5			20,758.3			20.7	
14	NULM	ND4L	2/2			9,810.9			9.9	
Sum						264,905.9				
Accessory nuclear coded										
15	NUEM	0/0	MNSFEN[g]	42,705.8	40,434.0	NADPH	745.4	40.4	R4	
16	ST1	0/0			34,621.2			34.5	R5	
17	NESM	1/0	FALRAY[g]	28,435.9	23,438.1			23.4		
18	NUJM	3/3			20,827.6			20.7	R6	
19	NUZM	0/0	MLPGGP[g]		19,749.6			19.7		
20	NUPM	0/0		19,327.2	19,196.0			19.2		

21	NUXM	3/2			18,565.2			18.5	
22	N7BM	0/0			16,153.2			16.1	
23	NUYM	0/0	QKKDVP[g]	18,671.1	15,939.9			15.9	
24	NUFM	0/0	NVSKGV[g]	16,635.0	15,572.7			15.6	
25	NIAM	1/1	IRASFD[g]	17,306.6	14,642.3			14.7	
26	NB4M	0/0	AIIATA[g]	14,757.8	14,626.7			14.6	
27	NUMM	0/0			14,257.0			14.4	
28	NB6M	1/1		14,091.4	13,960.2			13.9	R7
29	NUNM	1/1		15,794.8	13,300.9			13.4	
30	NI2M	0/0			12,879.8			12.8	
31	NB8M	0/0	AEFPPL[g]	1,119.0	11,067.8			11.1	R8
32	NIDM	0/0		11,021.3	10,890.1			10.9	
33	NB5M	1/1	VELKPS[g]	10,478.9	10,347.7			10.3	
34	ACPM2	0/0		14,428.5	9,526.7	PP-HD[e]	564.7	10.1	
35	NIPM	0/0			10,018.6			10.1	
36	NIMM	1/1		9,793.3	9,662.1			9.6	
37	ACPM1	0/0		12,040.6	9,071.2	PP-HD[e]	564.7	9.6	
38	NI8M	0/0		9,604.0	9,472.8			9.5	
39	NEBM	1/1		7,836.0	7,917.2			7.9	
40	NI9M	1/1		7,836.0	7,704.8			7.7	
41	NB2M	1/1		6,935.9	6,804.7			6.8	
Sum					410,648.1		1,874.8		R9

Remarks:
R1: NADH oxidation site
R2: Ubiquinone reduction site
R3: Catalytic core of complex I (coupling ubiquinone reduction to proton translocation)
R4: NADPH serves a structural role only (Abdrakhmanova et al. 2006)
R5: Confers in vitro thiosulfate:cyanide sulfurtransferase activity (Abdrakhmanova et al. 2005)
R6: Related to Tim17, Tim22 and Tim23 proteins involved in protein translocation across the inner mitochondrial membrane (Carroll et al. 2002)

(continued)

Table 2 (continued)

Subunit					M_r[c]		Prosth. groups		LILBID	
No	Gene	Protein	TMDs[a]	N-terminal sequence[b]	Precursor	Mature	Type	M_r	m/z	Remarks

R7: The mammalian homologue is identical to GRIM19, a protein implicated in interferon-β and retinoic acid-induced apoptotic cell death (Lufei et al. 2003; Huang et al. 2004)

R8: The human homologue displays structural similarity to thioredoxin-like ferredoxins (Brockmann et al. 2004)

R9: The total molecular mass of all constituent proteins is 949,649.4 Da; including all known prosthetic groups, the total molecular mass of complex I is 954,442.4 Da

[a]Predicted using servers http://www.enzim.hu/hmmtop/ and http://www.cbs.dtu.dk/services/TMHMM/

[b]Identified by Edman degradation

[c]Average molecular masses of mature proteins, calculated using the "compute pI/Mw" tool at http://www.expasy.ch/tools/pi_tool.html

[d]Including hexa-histidine tag and hexa-alanine spacer (Kashani-Poor et al. 2001a)

[e]Phosphopantetheine-hydroxy-tetradecanoate

[f]Djafarzadeh et al. (2000)

[g]Abdrakhmanova et al. (2004)

fungal enzyme as a model system for mammalian complex I offers a number of advantages. Fungal complex I is more stable and more easily purified in active form. Also, it does allow site-directed mutagenesis not only of the nuclear coded central but also the accessory subunits, including the remodelling and in vitro analysis of genetic defects in human complex I (see below).

2D and 3D models for the overall shape of complex I have been constructed by averaging electron microscopic pictures of single particles. While the resolution of this method is limited, the most detailed three-dimensional pictures by using this method were obtained using purified *Y. lipolytica* complex I (Clason et al. 2007). The two arms of complex I from several bacterial or eukaryotic sources have been dissociated using detergents or chaotropic reagents and then purified or further split into subcomplexes. Low-resolution images of fragments corresponding to the peripheral and the membrane intrinsic arm of *N. crassa* complex I have been published as early as 1991 (Hofhaus et al. 1991).

Before of high-resolution structural images of complex I became available, the X-ray structures of evolutionary-related enzymes, namely, the water-soluble [NiFe] hydrogenases from several eu- and archaebacterial sources (Montet et al. 1997) proved to be valuable models for the part of complex I that harbours the catalytic core of the enzyme, a designation we introduced for the domains immediately involved in the reduction of the quinone substrate and in coupling this reaction to proton translocation across the respiratory membrane (Kashani-Poor et al. 2001b). Bacterial [NiFe] hydrogenases consist of a large and a small subunit. They are related to the 49-kDa and PSST subunits of complex I, respectively. By generating a large number of amino acid substitutions in complex I of *Y. lipolytica* and assessing their effects on catalytic activity, inhibitor sensitivity and the electron paramagnetic resonance (EPR) signature of iron–sulfur cluster N2 (Ahlers et al. 2000b; Kashani-Poor et al. 2001b; Grgic et al. 2004; Garofano et al. 2003), we reached the following conclusions: The overall structure of the complex I catalytic core, located at the interface between the 49-kDa and PSST subunits, is highly similar to the corresponding part of bacterial [NiFe] hydrogenases. Iron–sulfur cluster in the PSST subunit corresponds to the so-called proximal iron–sulfur cluster in the hydrogenase small subunit, while the quinone-binding site in the 49-kDa subunit corresponds to the hydrogen evolving [NiFe] centre in the hydrogenase large subunit (Brandt et al. 2005).

A wealth of complex I inhibitors have been identified and several attempts at classification have been made (Degli Esposti 1998; Friedrich et al. 1994). The fact that several mutations in the catalytic core region of complex I affected the affinity for representative inhibitors from classes A (DQA, 2-decyl-4-quinazolinyl amine) and B (rotenone) provided strong support for the hypothesis that all classes of complex I inhibitors and the hydrophobic substrate ubiquinone bind to overlapping domains within a common binding pocket, as proposed in an earlier study using direct competition assays (Okun et al. 1999).

Later, the X-ray structure of the peripheral arm of *Thermus thermophilus* complex I was solved (Sazanov and Hinchliffe 2006). In this structure, the redox prosthetic groups of complex I appear arranged in a chain starting with the

non-covalently bound FMN molecule in the 51-kDa subunit that serves as the direct oxidant of NADH. Electrons are then passed on via an unbranched chain of iron–sulfur clusters that starts with tetranuclear cluster N3 in the 51-kDa subunit and terminates with binuclear cluster N2 in the homologue of the PSST subunit of bovine complex I. Binuclear cluster N1c, which is found in some bacterial complexes I only, does not participate in electron transfer reactions and merely serves a structural role.

It should be noted that there is an ongoing controversy on the assignment of the intervening clusters to the EPR signals that contribute to the EPR signatures. The "traditional" assignments, largely based on the work of Ohnishi and co-workers (Ohnishi 1998; Sazanov and Hinchliffe 2006), was recently challenged by Hirst and co-workers (Yakovlev et al. 2007; Roessler et al. 2010). While discussing this issue is beyond the scope of the present article, the "traditional" and "revised" assignments specific EPR signals to the iron–sulfur cluster bearing subunits of complex I are presented in Table 1.

The X-ray structure of the peripheral arm of *Th. thermophilus* complex I confirmed the notion that there is a high degree of structural similarity between bacterial [NiFe] hydrogenases and complex I. The interface between the 49-kDa and the PSST subunits, including the domains that correspond to [NiFe] cluster-binding site, forms a large cavity at the periphery of the fragment. It is widely accepted that this part of the enzyme constitutes much of the ubiquinone-binding pocket, within which the substrate has to interact with its specific binding site for productive interaction, i.e. reduction, coupled to proton pumping. Further research, including site-directed mutagenesis in *Y. lipolytica*, has provided a wealth of detailed information on this part of complex I (see below).

However, the position and orientation of the peripheral arm fragment and thus of the ubiquinone-binding pocket with respect to the membrane arm remained unclear. Also the involvement of the PSST subunits in crystal contacts and the fact that some sequence stretches within the 49-kDa and PSST subunits could not be resolved in the structure, left room for speculations on the actual shape and location of the ubiquinone-binding pocket within the holoenzyme. Meanwhile, the X-ray structural analysis of both the complete bacterial and mitochondrial complex I (Hunte et al. 2010; Efremov et al. 2010; Baradaran et al. 2013) revealed that the immediate electron donor of iron-sulfur cluster N2 resides about 30 Å above the polar headgroups of the membrane surface. This confirmed several lines of evidence indicating that this distance is at least 30 Å (Clason et al. 2007, 2010; Zickermann et al. 2003). In the structural models derived from these studies, the orientation of the quinone-binding pocket correctly suggested that it opens to the bulk phase and that the extremely hydrophobic substrate has to leave the membrane level at least in part. Clearly, the X-ray structure of the complex I holoenzyme was required to unambigously elucidate the orientation of the peripheral arm with respect to the membrane arm.

4 A Genetic Approach to *Y. lipolytica* Complex I

In the following, we report on our efforts to establish *Y. lipolytica* as a model system for the genetic and proteomic analysis of complex I. Through long years of spadework, a wealth of information has been obtained and a number of methodological approaches have been developed that now allow tackling various aspects of complex I structure, function and assembly.

All seven nuclear genes encoding the central subunits of the peripheral arm of complex I, as well as several others, could be cloned by virtue of sequence similarity with their homologues in fungi like *N. crassa* and in mammals. Following completion of the *Y. lipolytica* genome project, in addition to the seven nuclear coded central, a total of 27 genes for accessory subunits of *Y. lipolytica* complex I have been identified up to now (Table 2). Evidence that the protein products of these genes are bona fide subunits of *Y. lipolytica* complex I has been provided by proteomic analysis of the purified enzyme. For a subset of genes, including all seven central nuclear encoded subunits, deletion by homologous recombination was achieved, which either completely abolished complex I assembly or resulted in the appearance of subcomplexes that most likely represent relatively stable assembly intermediates (unpublished results).

As discussed above, the generation of strains carrying deletions of individual genes for complex I subunits was only achieved after genomic integration of the artificial NDH2i gene, encoding an internal version of alternative NADH dehydrogenase. Following replacement of the genomic copy of the NUGM gene encoding the 30-kDa subunit of complex I with a version carrying a C-terminally attached His-tag, affinity purification of *Y. lipolytica* complex I could be achieved with high purity and yield. To our best knowledge, this method holds the record for the largest multiprotein assembly purified to date using a single affinity tag.

However, strain development is still an ongoing process. For example, it can be expected that deletions of genes encoding complex I specific assembly factors or chaperones will yield intermediate phenotypes, i.e. result in an incomplete loss of complex I function. In such cases, it would be desirable to carry out suppressor or enhancer screens. This and other approaches will involve classical genetic crosses, employing truly isogenic strains. Such analyses are plagued with low mating and sporulation frequencies, low spore viabilities and non-uniform genetic background of the available *Y. lipolytica* strains. It has long been speculated that there is a common reason behind these problems: Multiple genomic rearrangements between individual “wild-type” isolates might prevent isogenisation by standard inbreeding programmes. An additional problem is presented by the fact that the frequency of homologous recombination is comparably low in *Y. lipolytica*, with the vast majority of recombinants resulting from random integration events.

Recently, we have put some effort into improving this situation. First, we deleted the homologue of the *N. crassa* mus51 gene (YALI0C08701g). In strains lacking this central component of the non-homologous end joining (NHEJ) system, a strong prevalence of homologous recombination repair (HRR) was observed following

transformation: a linear DNA fragment containing a *URA3* (gene encoding orotidine-5′-phosphate decarboxylase) marked deletion of a gene for an accessory complex I subunit was integrated by homologous recombination with the genomic locus in 12 out of 12 cases, a figure which is in stark contrast to the 0.25–12.5 % of homologous recombination events that we achieved in similar gene deletion projects using standard laboratory strains of *Y. lipolytica* (unpublished observation).

To generate truly isogenic strains of *Y. lipolytica*, we have replaced the mating-type locus from MATA to MATB in a YALI0C08701g deletion strain using pop-in-pop-out recombination. However, the project has not been finished yet, and mating and sporulation frequencies of strains isogenised by this "sex-reversal" procedure are yet unknown.

5 The Mitochondrial Genome of *Y. lipolytica*

In *Y. lipolytica*, like in mammals, the seven central, highly hydrophobic subunits of the membrane arm of complex I are encoded by the mitochondrial genome. Cross-hybridisation of a *Podospora anserina* mitochondrial DNA (mtDNA) probe with *Y. lipolytica* total DNA (Nosek and Fukuhara 1994) was among the first pieces of evidence for the presence of complex I in this obligate aerobic yeast; the sequence of a 6.6-kb *Y. lipolytica* mtDNA fragment containing the ND4 gene was published shortly afterwards (Matsuoka et al. 1994). The complete sequence of the *Y. lipolytica* mitochondrial genome could be determined at an early stage of the *Y. lipolytica* genome project by combining sequence information from a total DNA "shotgun" library and from contigs obtained by cloning of "satellite" DNA purified using cesium chloride gradient ultracentrifugation (Kerscher et al. 2001a).

Fourteen respiratory chain proteins are encoded by the *Y. lipolytica* mtDNA sequence, including the seven hydrophobic subunits (ND1-6 and ND4L) of the membrane arm of NADH:ubiquinone oxidoreductase (complex I), apocytochrome *b* of the cytochrome bc_1 complex (complex III), three subunits (COX1, 2, 3) of cytochrome *c* oxidase (complex IV) and three subunits of ATP synthase (complex V). N-terminal sequencing of several mitochondrial respiratory chain proteins clearly demonstrated that the *Y. lipolytica* mitochondrial genome is translated according to the "mold mitochondrial" translation table. However, up to date (February 2010), the NCBI database erroneously assigns "Translation table 3 (Yeast Mitochondrial)" as mitochondrial genetic code of *Y. lipolytica*.

The two RNA components of the mitochondrial ribosomes and 27 mitochondrial tRNAs were also found. The analysis of the *Y. lipolytica* mtDNA sequence revealed some unexpected features: the set of mitochondrial tRNAs is incomplete there is no tRNA able to read GCN codons encoding arginine, and, as a consequence, such codons are absent from the protein coding genes listed above. A total of 17 introns were found in the mitochondrial genome of *Y. lipolytica*. All of them fall into class I of fungal introns, characterised by a common secondary structure, a unique splicing

mechanism and the presence (at least in the majority of cases) of intronic open reading frames encoding endonucleases/maturases which may assist in the splice process or in "homing" into cognate intronless alleles. In the case of the *Y. lipolytica* mitochondrial genome, most of these intronic ORFs must be regarded as functionless pseudogenes, either because they have accumulated multiple frameshift and/or point mutations or because they contain untranslatable CGN codons.

6 A Proteomic Approach to *Y. lipolytica* Complex I

Mitochondrial membranes and purified complex I from *Y. lipolytica* were characterised extensively using several types of two-dimensional polyacrylamide gel electrophoresis (Abdrakhmanova et al. 2004, 2005; Djafarzadeh et al. 2000). For mitochondrial membranes, a combination of blue native polyacrylamide electrophoresis (BN-PAGE) and denaturing sodium dodecyl sulfate (SDS-PAGE) separation was routinely employed for assessing complex I assembly in strains carrying specific point mutation or gene deletions, as silver staining or Western blotting of such gels permits the detection of fully assembled complex I and subcomplexes that may either represent assembly intermediates or degradation products. Supercomplexes that contain complex I are also detectable but are not well resolved by this method. Analysis of purified complex I by dSDS-PAGE (in which the "d" stands for "doubled"), a combination of denaturing electrophoretic separation in the absence and presence of 16 % urea (Rais et al. 2004), proved especially useful for disclosing its constituent proteins. Due to the large number of subunits, a complex pattern of protein spots could be observed. A typical example is shown in Fig. 2. Separation of protein mixtures by dSDS-PAGE results in a typical pattern, with hydrophobic proteins running above and highly acidic proteins below the diagonal that contains the bulk of the proteins. In the case of *Y. lipolytica* complex I, six of the seven highly hydrophobic proteins encoded by the mitochondrial genome produced clearly visible spots on silver-stained dSDS gels, while the small ND4L subunit was not detectable. Assignment of individual protein spots to the corresponding genes was a formidable task that required the extensive application of various proteomic methods, most notably tandem mass spectrometry. Also, N-terminal sequences of several subunits of *Y. lipolytica* complex I were determined using Edman degradation.

However, dSDS gels do not allow accurate determinations of subunit masses. At this point, valuable insights could be gained by applying the newly developed method called laser-induced liquid bead ion desorption (LILBID) mass spectrometry (Morgner et al. 2008). This method allows the determination of molecular masses of undigested proteins and even non-covalent multiprotein complexes. As a drawback, at least at the current stage of technical development, it provides only limited mass accuracy, but this is far outweighed by the fact that it works very well with membrane proteins and can be applied to protein mixtures of which only minimal amounts are required. LILBID spectrometry of purified *Y. lipolytica*

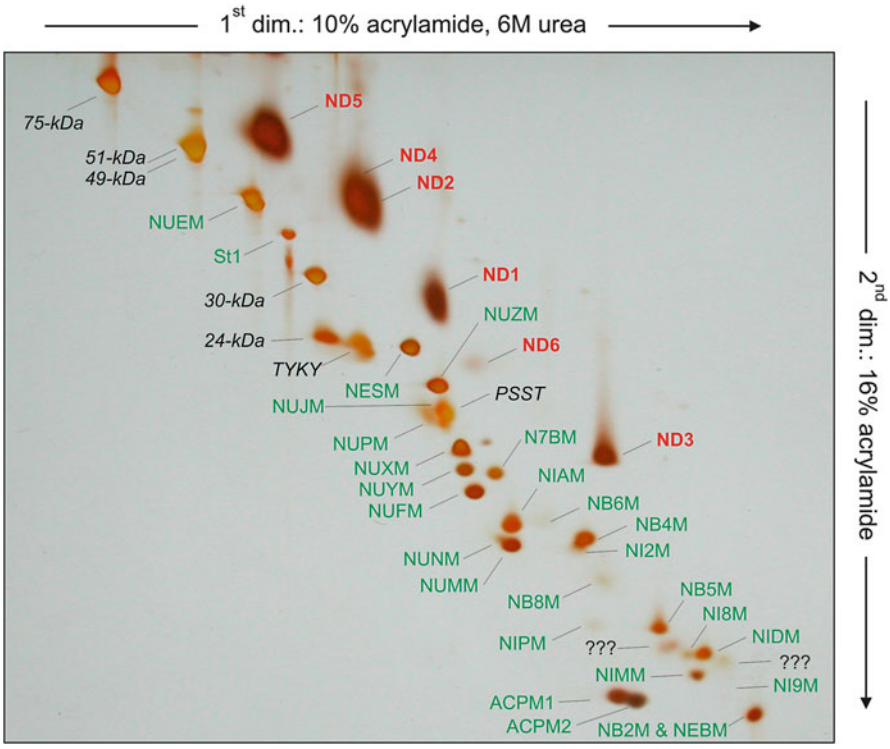

Fig. 2 dSDS-PAGE analysis of affinity-purified *Y. lipolytica* complex I. His-tagged complex I was purified using Ni-NTA Sepharose, followed by gel filtration on a TSK 4000SW column, separated on dSDS gels and stained with silver. Individual protein spots were cut out and subjected to tandem mass spectrometry. Hydrophobic, mitochondrially coded central subunits of the membrane arm (running above the diagonal) are labelled in *bold face*, hydrophilic central subunits of the peripheral arm in *italic* and accessory subunits of the peripheral arm in standard letters. All known subunits of *Y. lipolytica* complex I could be assigned to spots in the gel, with the sole exception of the small, mitochondrially coded ND4L protein. Two unidentified spots, most likely corresponding to contaminating proteins, are marked with "*question marks*"

complex I demonstrated that for seven of the small accessory subunits, peak positions were inconsistent with the masses deposited in the genome project. Careful searches for potential splice donor and acceptor sites in the corresponding genomic regions, followed by direct sequencing of cDNAs obtained by reverse transcription polymerase chain reaction (RT-PCR), indicated that the respective gene annotations had to be corrected.

All proteomic data on the 14 central and the 27 accessory subunits of *Y. lipolytica* complex I are summarised in Table 2. The roles of individual subunits in fungal and in mammalian complex I are listed as well—please note that as indicated part of this information is based on sequence similarities only and has not been confirmed experimentally. Especially, the function of most of the accessory subunits is not known. Among them, a group of small accessory subunits, all

possessing one transmembrane helix flanked by two highly charged domains, is remarkable. The number of such subunits seems to be highly variable between taxa, with 9 and 14 group members in *Y. lipolytica* and in mammals, respectively. Also, the degree of sequence similarity is rather low between taxa, and while some subunits can be assigned as homologues, their unifying feature seems to be functional analogy. We have speculated that these proteins, termed STMD (single transmembrane domain) subunits, function as assembly factors or chaperones but are retained in the fully assembled complex (Brandt et al. 2005; Zickermann et al. 2010). Interestingly, deletions of several of the corresponding genes (NIAM, NUNM, NB8M) resulted in similar complex I defects: only a very minor fraction of the enzyme was fully assembled, but the majority of the subunits, including all seven central subunits of the peripheral arm, were found within a large, membrane-associated subcomplex that migrated at an apparent molecular mass of about 700 kDa in BN-PAGE (unpublished results). A similar assembly defect was observed following deletion of the gene encoding the NUJM subunit, which has three transmembrane helices (unpublished results). In contrast, the STMD subunit NEBM seems to play a different role in complex I assembly. Following deletion of the NEBM gene, a hydrophobic subcomplex with a molecular mass of about 300 kDa was found (unpublished results). These observations support the notion that the STMD subunits, and the NUJM subunit, are involved in "joining" precursors of the peripheral and the membrane arm of complex I during assembly.

Although the proteomic analysis of *Y. lipolytica* complex I is now well advanced, we cannot be absolutely sure that all subunits have been identified. Both in the dSDS gel pattern and in the LILBID profile of *Y. lipolytica* complex I, a few unassigned features are apparent. These may represent additional, yet unidentified subunits of complex I or may arise from contaminating proteins, proteolytic breakdown or similar artefacts. However, by comparison of the subunits identified in *Y. lipolytica* with those identified in other fungi, we have reason to believe that our list is almost complete. For all subunits that were identified in complex I from *N. crassa*, the corresponding *Y. lipolytica* proteins could be identified, with one exception only: No counterpart for the NURM subunit of *N. crassa* (NCBI accession number: X71414) could be found so far in *Y. lipolytica*. Conversely, no counterpart of the *Y. lipolytica* NUNM gene (Genolevures accession number: YALI0F14003g) could be found in *N. crassa*. The fact that both genes encode STMD subunits seems to add further support to the hypothesis that there is little evolutionary conservation among this class of subunits.

Most of *Y. lipolytica* complex I seems to be present in mitochondrial membranes in monomeric form. Supercomplexes of respiratory chain complexes do occur as well but appear to be less frequent than in mammalian mitochondria (Nübel et al. 2009). In a careful study aimed at characterising complex I containing supercomplexes in mitochondrial membranes from *Y. lipolytica*, 2D BN gels were employed, using BN-PAGE as described in Wittig et al. (2006) in the first dimension and BN-PAGE with 0.02 % dodecyl-β-D-maltoside in the cathode buffer

Table 3 BN-PAGE of *Y. lipolytica* mitochondrial membranes reveals complex I in monomeric form or as part of supercomplexes

Band designation	Tentative composition	Apparent mass in BN-PAGE
I_1	I_1	950
d	I_1III_2 and I_1IV_2	1,400
e	$I_1III_2IV_1$	1,600
f	$I_1III_2IV_2$	1,800
⋆	I_1IV_1	1,150
♦	I_2	2,000

Adapted from Nübel et al. (2009)

in the second dimension. This analysis led to the identification of six such complexes, as summarised in Table 3 (Nübel et al. 2009).

A major advantage of the LILBID method is that it works with proteins eluted from BN-PAGE gels. Thus, LILBID has great potential for analysing the subunit composition of multiprotein complexes, including supercomplexes that are hard to purify with good yield and purity. This is illustrated by the fact that *Y. lipolytica* complex I prepared by the 2D BN-PAGE strategy described above is suitable for LILBID analysis (Sokolova et al. 2010). In the first dimension, using standard BN-PAGE, monomeric complex I is not well separated from dimeric complex V. In the second dimension, dimeric complex V is dissolved into monomers, and the complex I band can be excised. LILBID spectra of BN-PAGE bands were very similar to those obtained with affinity-purified complex I, but a few extra peaks were present as well which were most likely were due to complex V subunits. To identify such contaminating proteins more easily, LILBID spectra of dimeric *Y. lipolytica* complex V, isolated from BN gels in a similar fashion, were recorded (Sokolova et al. 2010). LILBID peaks could be assigned to 13 of the 15 complex V subunits identified by searching the *Y. lipolytica* genome. Again, in some cases, the splice pattern deposited in the genome project database had to be revised. The complex V data are summarised in Table 4.

7 Subunits Specific to *Y. lipolytica* Complex I

Thiosulfate:cyanide sulfurtransferase, also referred to as rhodanese, is an enzyme that is able to catalyse in vitro the transfer of a sulfane sulfur atom from thiosulfate to cyanide yielding thiocyanate and sulfite (Bordo and Bork 2002). While its in vivo function is still unknown, a number of physiological roles have been suggested, including involvement in the synthesis or repair of the iron–sulfur clusters of complex I (Pagani and Galante 1983; Ogata and Volini 1990).

Tandem mass spectrometric analysis demonstrated that rhodanese is present in *Y. lipolytica* complex I, purified by His-tag-mediated Ni^{2+}-affinity chromatography and gel filtration. The preparation exhibited a low level of in vitro rhodanese

Table 4 Subunits of *Y. lipolytica* complex V (ATP synthase)

ATP synthase subunit	Gene locus/gene name	Swiss-Prot/Uni-Prot	N-terminal sequence[a]	M_r		LILBID
				Precursor	Mature[b]	m/z
α	YALI0F03179g	Q6C326_YARLI	AEKATPEV[c]	58,078.64	55,407.47	55.5
β	YALI0B03982g	Q6CFT7_YARLI	ASSAGVGSGK[c]	54,406.97	50,894.76	51.0
γ	YALI0F02893g	Q6C338_YARLI	atLREIEMR[c]	32,336.8	30,074.18	30.1
b	YALI0F20306g	Q6C105_YARLI	sNQVDPKVKaT[c]	24,002.53	22,444.69	22.4
d	YALI0B06831g	Q6CFH9_YARLI	sVAAARSsAVK[c]	19,820.58	19,689.39	19.7
OSCP	YALI0D12584g	Q6C9B1_YARLI	ATKAAAPVKV[c]	22,776.33	20,518.47	20.5
h	YALI0F04774g	Q6C2V6_YARLI		11,636.89	9,456.33	9.5
ε	–	–	SAwKSAGFSF[d]	6,785.84	6,654.64	6.7
δ	YALI0D22022g	Q6C877_YARLI	AETASVDKLR[d,e]	17,349.51	14,720.38	14.7
i/j	YALI0D17490g	Q6C8S0_YARLI	aFGIRRAYPT[d]	6,941.05	6,809.86	6.8
g	YALI0B21527g	B5FVB8_YARLI	qstAASKAAS[d]	15,087.4	13,261.25	
e	YALI0E32164g	B5FVG3_YARLI	satLNVLR[d]	9,989.39	9,858.2	9.9
8	ATP8[f]	ATP8_YARLI	mPQLvPFyFT[d]	–	5,771.89	5.8
c	ATP9[f]	ATP9_YARLI	mQLvLA[d]	–	7,716.34	7.7
a	ATP6[f]	ATP6_YARLI		–	27,808.24	

[a]Identified by Edman degradation of Coomassie-stained bands on PVDF membranes
[b]Without posttranslational modifications
[c]From Nübel et al. (2009)
[d]From Sokolova et al. (2010)
[e]Under deformylation conditions
[f]Genes published in Kerscher et al. (2001a)

activity (Abdrakhmanova et al. 2005). These observations provided the first evidence that rhodanese forms a subunit of respiratory chain complex I. However, it seems that rhodanese is bound more loosely than other subunits, as it dissociates from the enzyme during BN-PAGE. Most likely, this interaction is even weaker and could therefore not be detected in other model systems. A genomic deletion of the *Y. lipolytica* rhodanese gene did not result in a detectable complex I defect (Abdrakhmanova et al. 2005). Activity and assembly of complex I appeared unchanged with respect to the parental strain, demonstrating that whatever in vivo function rhodanese may have, it is not essential for survival, at least under standard laboratory conditions.

Another unexpected finding with *Y. lipolytica* complex I was the presence of two subunits that are isoforms of ACPM (Dobrynin et al. 2010), mitochondrial proteins that exhibit strong sequence similarity to acyl carrier proteins, subunits of the prokaryotic type fatty acid synthase complex. In contrast, complex I from all other model systems analysed so far contains one ACPM subunit only (Cronan et al. 2005; Sackmann et al. 1991).

The function of the ACPM proteins remains elusive. However, homologues of the full set of enzymes involved in prokaryotic fatty acid synthesis have been detected in *S. cerevisiae* mitochondria (Hiltunen et al. 2005; Hiltunen et al. 2008), and several hypotheses regarding their functional roles have been put forward. These include de novo or repair synthesis of mitochondrial membrane phospholipids and synthesis of octanoic acid, a precursor of lipoic acid which acts as a redox prosthetic group in the pyruvate dehydrogenase and α-ketoglutarate dehydrogenase (Wada et al. 1997) complexes. Deletion of the genes encoding the two ACPM subunits of *Y. lipolytica* complex I also gave an unexpected result: while deletion of ACPM1 (locus name YALI0D14850g) interfered with proper assembly of complex I, deletion of ACPM2 (locus name YALI0D24629g) was incompatible with survival, indicating that this subunit, in addition to its function as a subunit of complex I, has an essential role in *Y. lipolytica* (Dobrynin et al. 2010).

8 Exploring Human Complex I Defects

Among inherited respiratory chain deficiencies, complex I deficiency is observed in many cases (Smeitink et al. 2004). A typical clinical presentation is Leigh syndrome, a severe, progressive neurodegenerative disease, with characteristic brainstem defects observed in magnetic resonance tomography (MRT) scans. A large number of mitochondrial mutations have been observed in Leigh syndrome patients, but point mutations in nuclear coded complex I subunits have also been described. In order to analyse their effects on catalytic activity, we have reconstructed several human complex I mutations using the *Y. lipolytica* system (Ahlers et al. 2000a). Mitochondrial membranes from mutant strains were isolated and their activities tested in vitro. By comparison with the enzyme from the parental strain, only rather small differences were observed. Even though great care has to

be applied when data obtained with the same enzyme from different organisms are to be compared, these results are plausible: Although human Leigh syndrome mutations have a lethal outcome, the fact that patients may survive for periods of time ranging from a few days to several years indicates that the resulting complex I defects are relatively mild. The positions of human Leigh syndrome mutations, using bacterial [NiFe] hydrogenases or the peripheral arm of *Th. thermophilus* complex I as structural models, are consistent with this view. Typically, they are found at a considerable distance from the catalytic core of complex I, at the periphery of the PSST and the 49-kDa subunits (Kerscher et al. 2004).

For a rather large fraction of Leigh syndrome patients, no mutations in complex I subunit genes could be identified, and it has been suspected that they may carry genetic defects affecting complex I specific assembly factors. Indeed, several such factors have been identified in recent years, either by the detection of the gene defects underlying familial Leigh or Leigh-like syndromes or by the identification of proteins associated with complex I or its assembly intermediates, followed by gene knockout or knockdown in a variety of model systems (Lazarou et al. 2009). The latter group constitute valuable candidate genes for elucidating the molecular defects underlying yet enigmatic cases of familial complex I defects.

Also, the method of evolutionary profiling has proven useful for the identification of complex I assembly factors. It is based on a comparison of the genetic inventories of a large number of organisms, confronting those that do possess complex I with those that do not. Genes present in most members of the first but absent in members of the second group may be regarded as candidates for complex I specific assembly factors. This approach led to the identification of the B17.2L protein, a paralogue of the complex I subunit B17.2 as a complex I specific chaperone, and to the identification of a patient with a progressive encephalopathy that carried a null mutation in the gene encoding B17.2L (Ogilvie et al. 2005).

A similar approach led to the identification of Ind1, a protein specifically required for the assembly of the iron–sulfur clusters of complex I. Gene deletion in *Y. lipolytica* (Bych et al. 2008) and siRNA-based knockdown in HeLa cells led to similar effects (Sheftel et al. 2009), demonstrating evolutionary conservation of this factor: In both cases, complex I content was reduced to bout 30 % of the original level, while other iron–sulfur cluster containing proteins, either residing in mitochondria or the cytosol, was largely unaffected.

9 Exploring the Reaction Mechanism of Complex I

The reaction mechanism of complex I is far from being understood. Two central questions have emerged in recent years: (1) how does the hydrophobic substrate ubiquinone bind and reach the active site and (2) how is electron transfer linked to proton translocation. These questions may be closely related. As discussed above, it has been shown that the orientation of the peripheral arm within the holoenzyme is such that the ubiquinone-binding site of complex I is situated about 30 Å above the

respiratory membrane (Hunte et al. 2010; Efremov et al. 2010; Baradaran et al. 2013). On the other hand, ubiquinone is a highly hydrophobic molecule that partitions almost quantitatively into the membrane phase. To reconcile this apparent contrast, we have postulated early on that a hydrophobic access path or "ramp" connects the membrane with the ubiquinone reduction site (Zickermann et al. 2003, 2009).

Evidence from our previous mutational analyses in *Y. lipolytica*, guided by the [NiFe] hydrogenase model, indicated that reduction of the hydrophobic substrate ubiquinone takes place at the interface between the 49-kDa and PSST subunits and that several complex I inhibitors bind to the same region (Kerscher et al. 2001c). This picture could be refined in a further round of mutagenesis, this time guided by the X-ray structure of the peripheral arm of *Th. thermophilus* complex I (Tocilescu et al. 2007; Fendel et al. 2008). In this work, for all amino acids with surface-exposed side chains in the proposed quinone-binding pocket of the *Th. thermophilus* enzyme, substitutions at the corresponding positions were created in *Y. lipolytica* complex I.

This round of mutagenesis yielded a number of interesting insights: The quinone-binding pocket of complex I has the shape of a funnel with a rather wide opening that is formed by the 49-kDa and PSST subunits, tapering into a narrow cleft formed by the interface of the two subunits, and terminates near iron–sulfur cluster N2 in the PSST subunit and the highly conserved Y144 residue in the 49-kDa subunit. The fact that even the most subtle change affecting the highly conserved Y144 residue in the 49-kDa subunit, namely, the Y144F replacement that merely removes the hydroxyl group, completely abolishes catalytic activity with the substrate analogue DBQ (*n*-decyl-ubiquinone) strongly suggests that this residue plays a key role in the catalytic cycle (Tocilescu et al. 2010). Complex I assembly and iron–sulfur cluster N2 EPR signals were unaffected by this and several other mutations at the same position. A more detailed analysis of the effects of the Y144F exchange became possible when it was discovered that complex I from this mutant displayed marked activity with the substrate analogues Q_1 and Q_2. The most likely explanation for this finding is that these molecules still bind to the ubiquinone reduction site. Although their hydrophobic side chains are shorter, their isoprene units may provide additional binding interactions allowing productive binding to the enzyme that is not feasible with the simple aliphatic side chain of DBQ.

Affinities for DQA and rotenone were dramatically decreased, indicating that Y144 plays a key role in the binding of inhibitors and the substrate ubiquinone. We propose that Y144 directly interacts with the headgroup of ubiquinone, most likely via a hydrogen bond between the aromatic hydroxyl and the ubiquinone carbonyl, placing the substrate in an ideal distance to its electron donor, iron–sulfur cluster N2. However, proton pumping still takes place with unchanged stoichiometry in complex I from the Y144F mutant, clearly demonstrating that Y144 is not involved in proton pumping (Tocilescu et al. 2010).

The nature of the proton pump of complex I is still unknown. Since cluster N2 of bovine heart complex I displays a marked redox-Bohr effect in the physiological pH range, it had been postulated that this cluster could be involved in proton

translocation. This hypothesis, however, was ruled out using the H226M mutation in the 49-kDa subunit of *Y. lipolytica* complex I (Zwicker et al. 2006). Mutating this highly conserved residue abolished the redox-Bohr properties of cluster N2 that resides in the immediate vicinity of H226. In the *Th. thermophilus* structure, the corresponding residue had been shown to form a hydrogen bond to cluster N2. However, in the H226M mutant, proton pumping was unaffected and occurred with unchanged stoichiometry, as shown by measurements using purified complex I reconstituted into proteoliposomes.

These observations led us to conclude that all proton pumping in complex I has to be coupled to the reduction of ubiquinone, which occurs in two steps, via formation of a semiquinone. It seems feasible that this highly charged intermediate has to bind to the active site in a conformation that differs from that in the presence of the uncharged substrate or product molecules and that an energetic barrier has to be passed for the required conformational rearrangement to occur at the substrate binding site (Zickermann et al. 2009). However, the question how this mechanism triggers proton translocation remains open. While their homology to Na^+/H^+ antiporters strongly suggests the ND2, ND4 and ND5 subunits of the membrane arm as constituents of the proton pump (Mathiesen and Hägerhall 2003), it is not easy to explain how conformational changes at the site of ubiquinone reduction could be transmitted across such distances. It is tempting to speculate that domains of several subunits, encoded by both the mitochondrial and the nuclear genomes, may serve as transmitter and trigger to drive the proton pump of complex I. Thus, at least some of these domains should be amenable to site-directed mutagenesis in *Y. lipolytica*.

Future work, involving a combination of experimental approaches to address both the number and location of semiquinone species and the conformational changes within the complex I catalytic cycle, will be required to clarify this matter.

References

Abdrakhmanova A, Zickermann V, Bostina M, Radermacher M, Schägger H, Kerscher S, Brandt U (2004) Subunit composition of mitochondrial complex I from the yeast *Yarrowia lipolytica*. Biochim Biophys Acta 1658:148–156

Abdrakhmanova A, Dobrynin K, Zwicker K, Kerscher S, Brandt U (2005) Functional sulfurtransferase is associated with mitochondrial complex I from *Yarrowia lipolytica*, but is not required for assembly of its iron-sulfur clusters. FEBS Lett 579:6781–6785

Abdrakhmanova A, Zwicker K, Kerscher S, Zickermann V, Brandt U (2006) Tight binding of NADPH to the 39-kDa subunit of complex I is not required for catalytic activity but stabilizes the multiprotein complex. Biochim Biophys Acta 1757:1676–1682

Ahlers P, Garofano A, Kerscher S, Brandt U (2000a) Application of the obligate aerobic yeast *Yarrowia lipolytica* as a eukaryotic model to analyze Leigh Syndrome mutations in the complex I core subunits PSST and TYKY. Biochim Biophys Acta 1459:258–265

Ahlers P, Zwicker K, Kerscher S, Brandt U (2000b) Function of conserved acidic residues in the PSST-homologue of complex I (NADH:ubiquinone oxidoreductase) from *Yarrowia lipolytica*. J Biol Chem 275:23577–23582

Arthur H, Watson K (1976) Thermal adaptation in yeasts: growth temperatures, membrane lipid, and cytochrome composition of psychrophilic, mesophilic, and thermophilic yeasts. J Bacteriol 128:56–68

Baradaran R, Berrisford JM, Minhas GS, Sazanov LA (2013) Crystal structure of the entire respiratory complex I. Nature 494:443–448

Barth G, Gaillardin C (1996) *Yarrowia lipolytica*. In: Wolf K (ed) Non-conventional yeasts in biotechnology. Springer, Heidelberg, pp 313–388

Bordo D, Bork P (2002) The rhodanese/Cdc25 phosphatase superfamily – sequence-structure-function relations. EMBO Rep 3:741–746

Brandt U (2006) Energy converting NADH: quinone oxidoreductase (complex I). Annu Rev Biochem 75:69–92

Brandt U, Abdrakhmanova A, Zickermann V, Galkin A, Dröse S, Zwicker K, Kerscher S (2005) Structure–function relationships in mitochondrial complex I of the strictly aerobic yeast *Yarrowia lipolytica*. Biochem Soc Trans 33:840–844

Brockmann C, Diehl A, Rehbein K, Strauss H, Schmieder P, Korn B, Kuhne R, Oschkinat H (2004) The oxidized subunit B8 from human complex I adopts a thioredoxin fold. Structure 12:1645–1654

Bych K, Kerscher S, Netz DJ, Pierik AJ, Zwicker K, Huynen MA, Lill R, Brandt U, Balk J (2008) The iron-sulphur protein Ind1 is required for effective complex I assembly. EMBO J 27:1736–1746

Carroll J, Shannon RJ, Fearnley IM, Walker JE, Hirst J (2002) Definition of the nuclear encoded protein composition of bovine heart mitochondrial complex I – identification of two new subunits. J Biol Chem 277:50311–50317

Carroll J, Fearnley IM, Skehel JM, Shannon RJ, Hirst J, Walker JE (2006) Bovine complex I is a complex of 45 different subunits. J Biol Chem 281:32724–32727

Clason T, Zickermann V, Ruiz T, Brandt U, Radermacher M (2007) Direct localization of the 51 and 24 kDa subunits of mitochondrial complex I by three-dimensional difference imaging. J Struct Biol 159:433–442

Clason T, Ruiz T, Schagger H, Peng G, Zickermann V, Brandt U, Michel H, Radermacher M (2010) The structure of eukaryotic and prokaryotic complex I. J Struct Biol 169:81–88

Cronan JE, Fearnley IM, Walker JE (2005) Mammalian mitochondria contain a soluble acyl carrier protein. FEBS Lett 579:4892–4896

Degli Esposti M (1998) Inhibitors of NADH-ubiquinone reductase: an overview. Biochim Biophys Acta 1364:222–235

Djafarzadeh R, Kerscher S, Zwicker K, Radermacher M, Lindahl M, Schägger H, Brandt U (2000) Biophysical and structural characterization of proton-translocating NADH-dehydrogenase (complex I) from the strictly aerobic yeast *Yarrowia lipolytica*. Biochim Biophys Acta 1459:230–238

Dobrynin K, Abdrakhmanova A, Richers S, Hunte C, Kerscher S, Brandt U (2010) Characterization of two different acyl carrier proteins in complex I from *Yarrowia lipolytica*. Biochim Biophys Acta 1797:152–159

Dujon B, Sherman D, Fischer G, Durrens P, Casaregola S, Lafontaine I, de Montigny J, Marck C, Neuveglise C, Talla E, Goffard N, Frangeul L, Aigle M, Anthouard V, Babour A, Barbe V, Barnay S, Blanchin S, Beckerich JM, Beyne E, Bleykasten C, Boisrame A, Boyer J, Cattolico L, Confanioleri F, De Daruvar A, Despons L, Fabre E, Fairhead C, Ferry-Dumazet H, Groppi A, Hantraye F, Hennequin C, Jauniaux N, Joyet P, Kachouri R, Kerrest A, Koszul R, Lemaire M, Lesur I, Ma L, Muller H, Nicaud JM, Nikolski M, Oztas S, Ozier-Kalegeropoulos O, Pellenz S, Potier S, Richard GF, Straub ML, Suleau A, Swennen D, Tekaia F, Wesolowski-Louvel M, Westhof E, Wirth B, Zeniou-Meyer M, Zivanovic I, Bolotin-Fukuhara M, Thierry A, Bouchier C, Caudron B, Scarpelli C, Gaillardin C, Weissenbach J, Wincker P, Souciet JL (2004) Genome evolution in yeasts. Nature 430:35–44

Efremov RG, Baradaran R, Sazanov LA (2010) The architecture of respiratory complex I. Nature 465:441–445

Fendel U, Tocilescu MA, Kerscher S, Brandt U (2008) Exploring the inhibitor binding pocket of respiratory complex I. Biochim Biophys Acta 1777:660–665

Friedrich T (1998) The NADH:ubiquinone oxidoreductase (complex I) from *Escherichia coli*. Biochim Biophys Acta 1364:134–146

Friedrich T, Ohnishi T, Forche E, Kunze B, Jansen R, Trowitzsch W, Hofle G, Reichenbach HX, Weiss H (1994) Two binding sites for naturally occurring inhibitors in mitochondrial and bacterial NADH:ubiquinone oxidoreductase (complex I). Biochem Soc Trans 22:226–230

Galkin AS, Grivennikova VG, Vinogradov AD (2001) $H^+/2e^-$ stoichiometry of the NADH: ubiquinone reductase reaction catalyzed by submitochondrial particles. Biochemistry (Mosc) 66:435–443

Galkin A, Dröse S, Brandt U (2006) The proton pumping stoichiometry of purified mitochondrial complex I reconstituted into proteoliposomes. Biochim Biophys Acta 1757:1575–1581

Garofano A, Zwicker K, Kerscher S, Okun P, Brandt U (2003) Two aspartic acid residues in the PSST-homologous NUKM subunit of complex I from *Yarrowia lipolytica* are essential for catalytic activity. J Biol Chem 278:42435–42440

Grgic L, Zwicker K, Kashani-Poor N, Kerscher S, Brandt U (2004) Functional significance of conserved histidines and arginines in the 49 kDa subunit of mitochondrial complex I. J Biol Chem 279:21193–21199

Hiltunen JK, Okubo F, Kursu VAS, Autio KJ, Kastaniotis AJ (2005) Mitochondrial fatty acid synthesis and maintenance of respiratory competent mitochondria in yeast. Biochem Soc Trans 33:1162–1165

Hiltunen JK, Schonauer MS, Kaija JA, Mittelmeier TM, Kastaniotis AJ, Dieckmann CL (2008) Mitochondrial fatty acid synthesis type II: more than just fatty acids. J Biol Chem 284:9011–9015

Hofhaus G, Weiss H, Leonard K (1991) Electron microscopic analysis of the peripheral and membrane parts of mitochondrial NADH dehydrogenase (complex I). J Mol Biol 221:1027–1043

Huang GC, Lu H, Hao AJ, Ng DCH, Ponniah S, Guo K, Lufei CC, Zeng Q, Caoj XM (2004) GRIM-19, a cell death regulatory protein, is essential for assembly and function of mitochondrial complex I. Mol Cell Biol 24:8447–8456

Hunte C, Zickermann V, Brandt U (2010) Functional modules and structural basis of conformational coupling in mitochondrial complex I. Science 329:448–451

Joseph-Horne T, Hollomon DW, Wood PM (2001) Fungal respiration: a fusion of standard and alternative components. Biochim Biophys Acta 1504:179–195

Kashani-Poor N, Kerscher S, Zickermann V, Brandt U (2001a) Efficient large scale purification of his-tagged proton translocating NADH : ubiquinone oxidoreductase (complex I) from the strictly aerobic yeast *Yarrowia lipolytica*. Biochim Biophys Acta 1504:363–370

Kashani-Poor N, Zwicker K, Kerscher S, Brandt U (2001b) A central functional role for the 49-kDa subunit within the catalytic core of mitochondrial complex I. J Biol Chem 276:24082–24087

Kerscher S (2000) Diversity and origin of alternative NADH:ubiquinone oxidoreductases. Biochim Biophys Acta 1459:274–283

Kerscher S, Okun JG, Brandt U (1999) A single external enzyme confers alternative NADH: ubiquinone oxidoreductase activity in *Yarrowia lipolytica*. J Cell Sci 112:2347–2354

Kerscher S, Durstewitz G, Casaregola S, Gaillardin C, Brandt U (2001a) The complete mitochondrial genome of *Yarrowia lipolytica*. Comp Funct Genomics 2:80–90

Kerscher S, Eschemann A, Okun PM, Brandt U (2001b) External alternative NADH:ubiquinone oxidoreductase redirected to the internal face of the mitochondrial inner membrane rescues complex I deficiency in *Yarrowia lipolytica*. J Cell Sci 114:3915–3921

Kerscher S, Kashani-Poor N, Zwicker K, Zickermann V, Brandt U (2001c) Exploring the catalytic core of complex I by *Yarrowia lipolytica* yeast genetics. J Bioenerg Biomembr 33:187–196

Kerscher S, Grgic L, Garofano A, Brandt U (2004) Application of the yeast *Yarrowia lipolytica* as a model to analyse human pathogenic mutations in mitochondrial complex I. Biochim Biophys Acta 1659:197–205

Kurtzman CP (1994) Molecular taxonomy of the yeasts. Yeast 10:1727–1740

Lagunas R (1986) Misconceptions about the energy metabolism of *Saccharomyces cerevisiae*. Yeast 2:221–228

Lazarou M, Thorburn DR, Ryan MT, McKenzie M (2009) Assembly of mitochondrial complex I and defects in disease. Biochim Biophys Acta 1793:78–88

Lufei C, Ma J, Huang G, Zhang T, Novotny-Diermayr V, Ong CT, Cao X (2003) GRIM-19, a death-regulatory gene product, suppresses Stat3 activity via functional interaction. EMBO J 22:1325–1335

Luttik MAH, Overkamp KM, Kötter P, de Vries S, van Dijken P, Pronk JT (1998) The *Saccharomyces cerevisiae NDE1 and NDE2* genes encode separate mitochondrial NADH dehydrogenases catalyzing the oxidation of cytosolic NADH. J Biol Chem 273:24529–24534

Marres CAM, de Vries S, Grivell LA (1991) Isolation and inactivation of the nuclear gene encoding the rotenone-insensitive internal NADH:ubiquinone oxidoreductase of mitochondria from *Saccharomyces cerevisiae*. Eur J Biochem 195:857–862

Mathiesen C, Hägerhall C (2003) The 'antiporter module' of respiratory chain Complex I includes the MrpC/NuoK subunit – a revision of the modular evolution scheme. FEBS Lett 549:7–13

Matsuoka M, Matsubara M, Inoue J, Kakehi M, Imanaka T (1994) Organization and transcription of the mitochondrial ATP synthase genes in the yeast *Yarrowia lipolytica*. Curr Genet 26:382–389

Medentsev AG, Akimenko VK (1999) Development and activation of cyanide-resistant respiration in the yeast *Yarrowia lipolytica*. Biochemistry 64:945–951

Melo AM, Bandeiras TM, Teixeira M (2004) New insights into type II NAD(P)H:quinone oxidoreductases. Microbiol Mol Biol Rev 68:603–616

Montet Y, Amara P, Volbeda A, Vernede X, Hatchikian EC, Field MJ, Frey M, Fontecilla-Camps JC (1997) Gas access to the active site of Ni-Fe hydrogenases probed by X-ray crystallography and molecular dynamics. Nat Struct Biol 4:523–526

Morgner N, Zickermann V, Kerscher S, Wittig I, Abdrakhmanova A, Barth HD, Brutschy B, Brandt U (2008) Subunit mass fingerprinting of mitochondrial complex I. Biochim Biophys Acta 1777:1384–1391

Nosek J, Fukuhara H (1994) NADH dehydrogenase subunit genes in the mitochondrial DNA of yeasts. J Bacteriol 176:5622–5630

Nübel E, Wittig I, Kerscher S, Brandt U, Schägger H (2009) Two-dimensional native electrophoretic analysis of respiratory supercomplexes from *Yarrowia lipolytica*. Proteomics 9(9): 2408–2418

Ogata K, Volini M (1990) Mitochondrial rhodanese – membrane-bound and complexed activity. J Biol Chem 265:8087–8093

Ogilvie I, Kennaway NG, Shoubridge EA (2005) A molecular chaperone for mitochondrial complex I assembly is mutated in a progressive encephalopathy. J Clin Invest 115:2784–2792

Ohnishi T (1998) Iron-sulfur clusters semiquinones in complex I. Biochim Biophys Acta 1364:186–206

Okun JG, Lümmen P, Brandt U (1999) Three classes of inhibitors share a common binding domain in mitochondrial complex I (NADH:ubiquinone oxidoreductase). J Biol Chem 274:2625–2630

Pagani S, Galante YM (1983) Interaction of rhodanese with mitochondrial NADH dehydrogenase. Biochim Biophys Acta 742:278–284

Radermacher M, Ruiz T, Clason T, Benjamin S, Brandt U, Zickermann V (2006) The three-dimensional structure of complex I from *Yarrowia lipolytica*: a highly dynamic enzyme. J Struct Biol 154:269–279

Rais I, Karas M, Schägger H (2004) Two-dimensional electrophoresis for the isolation of integral membrane proteins and mass spectrometric identification. Proteomics 4:2567–2571

Roessler MM, King MS, Robinson AJ, Armstrong FA, Harmer J, Hirst J (2010) Direct assignment of EPR spectra to structurally defined iron-sulfur clusters in complex I by double electron–electron resonance. Proc Natl Acad Sci USA 107:1930–1935

Sackmann U, Zensen R, Roehlen D, Jahnke U, Weiss H (1991) The acyl-carrier protein in *Neurospora crassa* mitochondria is a subunit of NADH: ubiquinone reductase (complex I). Eur J Biochem 200:463–469

Sazanov LA, Hinchliffe P (2006) Structure of the hydrophilic domain of respiratory complex I from *Thermus thermophilus*. Science 311:1430–1436

Sheftel AD, Stehling O, Pierik AJ, Netz DJA, Kerscher S, Elsasser HP, Wittig I, Balk J, Brandt U, Lill R (2009) Human Ind1, an iron-sulfur cluster assembly factor for respiratory complex I. Mol Cell Biol 29:6059–6073

Smeitink JAM, van den Heuvel LWPJ, Koopman WJH, Nijtmans LGJ, Ugalde C, Willems PHGM (2004) Cell biological consequences of mitochondrial NADH: ubiquinone oxidoreductase deficiency. Curr Neurovasc Res 1:29–40

Sokolova L, Wittig I, Barth HD, Schägger H, Brutschy B, Brandt U (2010) Laser-induced liquid bead ion desorption-MS of protein complexes from blue-native gels, a sensitive top-down proteomic approach. Proteomics 10:1401–1407

Tocilescu MA, Fendel U, Zwicker K, Kerscher S, Brandt U (2007) Exploring the ubiquinone binding cavity of respiratory complex I. J Biol Chem 282:29514–29520

Tocilescu MA, Fendel U, Zwicker K, Dröse S, Kerscher S, Brandt U (2010) The role of a conserved tyrosine in the 49-kDa subunit of complex I for ubiquinone binding and reduction. Biochim Biophys Acta 1797(6–7):625–632

Wada H, Shintani D, Ohlrogge J (1997) Why do mitochondria synthesize fatty acids? Evidence for involvement in lipoic acid production. Proc Natl Acad Sci USA 94:1591–1596

Wittig I, Braun HP, Schägger H (2006) Blue native PAGE. Nat Protoc 1:418–428

Yakovlev G, Reda T, Hirst J (2007) Reevaluating the relationship between EPR spectra and enzyme structure for the iron-sulfur clusters in NADH: quinone oxidoreductase. Proc Natl Acad Sci USA 104:12720–12725

Yano T, Yagi T (1999) H^+-translocating NADH-quinone oxidoreductase (NDH-1) of *Paracoccus denitrificans*. J Biol Chem 274:28606–28611

Zickermann V, Bostina M, Hunte C, Ruiz T, Radermacher M, Brandt U (2003) Functional implications from an unexpected position of the 49 kDa subunit of complex I. J Biol Chem 278:29072–29078

Zickermann V, Kerscher S, Zwicker K, Tocilescu MA, Radermacher M, Brandt U (2009) Architecture of complex I and its implications for electron transfer and proton pumping. Biochim Biophys Acta 1787:574–583

Zickermann V, Angerer H, Ding MG, Nübel E, Brandt U (2010) Small single transmembrane domain (STMD) proteins organize the hydrophobic subunits of large membrane protein complexes. FEBS Lett 584(12):2516–2525

Zwicker K, Galkin A, Dröse S, Grgic L, Kerscher S, Brandt U (2006) The redox-Bohr group associated with iron-sulfur cluster N2 of complex I. J Biol Chem 281:23013–23017

http://www.springer.com/978-3-642-38319-9

Yarrowia lipolytica
Genetics, Genomics, and Physiology
Barth, G. (Ed.)
2013, VII, 187 p., Hardcover
ISBN: 978-3-642-38319-9